Nuclear-plus-interference-scattering effect on the energy deposition of multi-MeV protons in a dense Be plasma

Zhigang Wang,[1] Zhenguo Fu,[1,2] Bin He,[1] Zehua Hu,[1] and Ping Zhang[1,*]
[1]*Institute of Applied Physics and Computational Mathematics, Beijing 100088, China*
[2]*Center for Fusion Energy Science and Technology, CAEP, Beijing 100088, China*
(Received 1 February 2016; revised manuscript received 23 April 2016; published 8 September 2016)

The nuclear plus interference scattering (NIS) effect on the stopping power of hot dense beryllium (Be) plasma for multi-MeV protons is theoretically investigated by using the generalized Brown-Preston-Singleton (BPS) model, in which a NIS term is taken into account. The analytical formula of the NIS term is detailedly derived. By using this formula, the density and temperature dependence of the NIS effect is numerically studied, and the results show that the NIS effect becomes more and more important with increasing the plasma temperature or density. Different from the cases of protons traveling through the deuterium-tritium plasmas, for a Be plasma, a prominent oscillation valley structure is observed in the NIS term when the proton's energy is close to $E_p = 7\,\mathrm{MeV}$. Furthermore, the penetration distance is remarkably reduced when the NIS term is considered.

DOI: 10.1103/PhysRevE.94.033205

I. INTRODUCTION

The problem of the stopping power of charged particles in dense plasmas is of considerable interest for many fields of modern physics, including astrophysics, fusion physics, condensed-matter physics, and other related fields [1]. Increasing efforts have been devoted to understanding the physical properties involved in the stopping power. As a consequence, many theoretical models for the stopping power have been developed. The first classical theoretical model about the energy loss of ions in matter may be proposed by Bohr in 1913 [2], followed by Bethe and Bloch using perturbative quantum-mechanical calculations [3]. Later, more elaborate approaches beyond the perturbation theory were also developed [4]. For example, Brown, Preston, and Singleton developed a dimensional continuation method, in which both short- and long-distance physics are taken into account by the Boltzmann and the Lenard-Balescu equations [5]. A method of coupled mode energy relaxation rate [6–9] has also been derived, in which the effects of particle screening, electron degeneracy, and correlations between electrons and ions are considered via local field corrections. This approach could be regarded as an extension of the Fermi golden rule approach [10], in which the dynamics of electronic and ionic subsystems are treated independently. By now, ion stopping in cold matter is relatively well understood with abundant experimental data and several available simulation codes [11,12].

However, because of various theoretical and experimental challenges, ion stopping in ionized plasmas is far from being understood. Only a few experimental data have been collected. The advanced progresses of the OMEGA laser facility at University of Rochester, USA [13–15], the PHELIX laser facility at GSI Helmholtzzentrum für Schwerionenforschung, Germany [16,17], and the ITEP facility at Institute for Theoretical and Experimental Physics, Russia [18] enable an investigation of the ion energy loss in a hot dense plasma. Recently, the stopping power of protons in a warm dense beryllium (Be) plasma with solid-density and an electron temperature of 32 eV has been measured successfully on the OMEGA laser facility [14]. The experimental data, in contrast, cannot be perfectly explained by the present theoretical models [4,5,19]. More recently, the stopping of ions produced in the nuclear reactions in weakly coupled fusion plasmas has also been quantitatively measured [15], and the experimental results generally support the predictions of the Brown-Preston-Singleton (BPS) [5] and Li-Petrasso models [19]. The diagnostics of plasmas with ions [20] are arising applications that require a good understanding of the beam-plasma interaction. In order to predict inertial confinement fusion (ICF) [21,22], the stopping power of dense plasma is one of many quantities that must be calculated accurately.

To our knowledge, most of the present models for the stopping power focus on the Coulomb scattering (CS) contributions, but many other important physical effects were ignored. Recently, the mixing effect of deuterium-tritium (DT) plasmas [13,23–30] with Be, gold, as well as uranium has been extensively studied [31–34]. DT neutron yield and ion temperature decrease abruptly when the hot spot mix mass increases above several hundred nanogram in the indirect-drive ICF experiments. It has also been found that the high-Z plasma from the inner side of the hohlraum blow-off results in low mode number implosion asymmetries [32]. During the ignition period of DT fuel in the indirect-driven ICF experiments, the energy loss of charged particles in the DT capsule should be influenced remarkably by the plasmas from the inner-side of hohlraum because of its admixture with DT plasma.

In addition, the nuclear plus interference scattering (NIS) effect should be very important during the implosion dynamics. This is because the experimental measured differential scattering cross sections for muti-MeV particles on nuclei mainly include three components: (i) the CS component, (ii) the nuclear scattering component, and (iii) the component denoting interference between these two processes. If one focuses on the analysis of collisional phenomena, the dominant process in the energy deposition of charged particles traveling in plasmas is the small-angle CS [15]. If the energy of the projected particle is high enough (multi-MeV) and the

*Corresponding author: zhang_ping@iapcm.ac.cn

temperature of the background hot dense plasma is relatively higher than several tens keV, however, the minimum distance can be of the order of the nuclear force range. At this condition, NIS will take place and the energy of the projected particle is deposited directly to the ion species in the background plasmas [35,36]. This is because the CS time is relatively long. Multi-MeV charged particles, such as the 14.6 MeV proton produced in the fusion reaction $D + {}^3\mathrm{He} \rightarrow {}^4\mathrm{He} + p$, can undergo several NIS collisions with the background ions before reaching thermal energies.

The CS constitutes the dominant energy deposition process, and is modeled by a large cross section and small energy transfer [5,15]. While the NIS is a *non-Coulombic*, large-energy-transfer scattering process. The effect of NIS on the energy deposition of several fast particles passing through a D plasma has been first studied by Devaney and Stein [37]. In the modern conceptual designs of next generation fusion devices, a particle-beam with energy of multi-MeV is considered to be used. For instance, the design of advanced fast ignition [38] experiments on upgraded facilities (OMEGA-EP, FIREX, and HIPER) [39–42] requires more accurate and realistic studies of energy deposition and ignition. In this case, the NIS effect on energy deposition of beam particles should not be ignored comparing with those due to CS. The stopping of fast electrons in fusion plasmas has been theoretically discussed [43–45]. Recently, Mahdavi and Koohrokhi [46] calculated the NIS effect on the energy loss and penetration of multi-MeV protons into a uniform DT plasma. The interaction of a quasi-monoenergetic proton beam with a pre-compressed inertial fusion fuels has also been studied based on a kinetic model including the effect of NIS [47]. The maximum proton energies above 85 MeV with high particle numbers has also been successfully realized in the most recent experiment [48]. With the advanced progress of the National Ignition Facility (NIF) [49–51], it is possible for the studies of hot dense plasmas with electron densities exceeding 10^{25} cm^{-3} and temperatures up to tens keV. These developments of techniques may give the possibility to study the NIS effect during the implosion in the future experiments.

As mentioned above, Be [52–57] is very important in ICF due to its appearance in the ablator of the DT capsule. Michel *et al.* reported that the implosion velocity of Be shells was increased by 20% compared to carbon and CH shells in direct-driven implosions [54]. Casey *et al.* found that indirect-driven Be implosions showed good performance on the average DD neutron yield [56]. Most recently, ICF targets with silicon layered between an inner Be (14 μm) and outer silicon-doped plastic ablator were used in the implosion experiments performed on the OMEGA laser facility. The experiments showed that a factor-of-5 reduction in hot-electron generation was observed in the multilayer targets relative to pure CH targets [57]. However, to our knowledge, there is little report about the NIS contribution to the stopping of protons in hot dense Be plasma. Because of the basic interest and the importance to the ICF experiments, it is a timely task to provide a theoretical analysis for the proton stopping power of the Be plasma in the presence of both the CS and NIS effect. Therefore, in this paper, we study the energy deposition of protons in the Be plasma by using the generalized BPS model, in which both the CS and NIS effects are considered.

The paper is organized as follows. In Sec. II we introduce the stopping power formulas used in this work. The formulas of calculating the CS term in the BPS model is simply given. Starting from the classical Boltzmann equation, we carefully derive the NIS part of the stopping power of charged particles, and the analytical expression is obtained. In Sec. III, based on the generalized BPS model given in the last section, we numerically calculate the stopping power for multi-MeV protons moving in the hot dense Be plasma with temperatures from 10 keV to 100 keV and number densities from 10^{24}cm^{-3} to 10^{27} cm^{-3}. Three main results are obtained: (i) the NIS effect becomes more and more important by increasing plasma temperature or density; (ii) a prominent oscillation valley is observed in the NIS term as a function of the proton's energy near $E_p = 7$ MeV; and (iii) the penetration distance of proton in the plasma is remarkably reduced when the NIS effect is considered at high plasma temperature and/or under dense plasma density. The relevant physical analyses are also given in this section. A summary is given in Sec. IV.

II. THE STOPPING POWER FORMULAS

The charged particles moving in the plasmas lose their energies in two ways: (i) by Coulomb collisions with background ions and electrons, and (ii) by nuclear scattering with ions. Furthermore, there exists interference between the Coulomb collisions and the nuclear scattering. In this work, we focus on the NIS effect on the stopping power of plasmas. The total stopping power is expressed as

$$\frac{dE}{dx} = \frac{dE^{\mathrm{Coul}}}{dx} + \frac{dE^{NI}}{dx}, \tag{1}$$

where $\frac{dE^{\mathrm{Coul}}}{dx} = (\frac{dE}{dx})_e^{\mathrm{Coul}} + \sum_{b\neq e}(\frac{dE}{dx})_b^{\mathrm{Coul}}$ is the CS term, and $\frac{dE^{NI}}{dx} = \sum_{b\neq e}(\frac{dE}{dx})_b^{NI}$ denotes the NIS one. The superscripts $Coul$ and NI refer to Coulomb and NIS contributions, respectively. The subscript $b = i,e$ refers to ion species and electron species in the plasma. The CS term is quite based on the BPS theory [5], which is given by $\frac{dE^{\mathrm{Coul}}}{dx} = \sum_b (\frac{dE^C_{b,S}}{dx} + \frac{dE^<_{b,R}}{dx} + \frac{dE^Q_b}{dx})$. The first term represents the classical short-distance contribution, the second term is the classical long-distance contribution, and the third term denotes the quantum correction to the classical part. For brevity, detailed expressions for each term are not given here, but can be found in Refs. [5] and [34]. Notice that the electrons and ions are considered as classical particles which obey the Maxwell-Boltzmann distribution, and the quantum correction herein becomes remarkable when the quantum Debye wavelength is much larger than the classical minimum approach distance. Otherwise, the contribution of $\frac{dE^Q_b}{dx}$ is too small to be omitted comparing with the classical parts.

In order to describe this process, the transport equation should include an additional Boltzmann collision term. Explicitly, the Boltzmann equation is given by

$$\left[\frac{\partial}{\partial t} + \boldsymbol{v}_p\right] f_p(\boldsymbol{r},\boldsymbol{p}_p,t) = \sum_b C_{pb}(\boldsymbol{r},\boldsymbol{p}_p,t). \tag{2}$$

Here, the NIS effects on the stopping power can be derived through generalizing the scattering integrals in the dynamical friction coefficient and the dispersion tensor to include the NIS differential cross section $\frac{d\sigma_{pb}^{NI}}{d\Omega}$. From the collision term, $C_{pb}(\boldsymbol{r},\boldsymbol{p}_p,t)$, one can get the stopping power of projectile due to NIS as the following form:

$$\frac{dE^{NI}}{dx} = -\sum_b \int \frac{d^3\boldsymbol{p}_b}{(2\pi\hbar)^3} v_{pb} f_b(\boldsymbol{p}_b) \int d\Omega (E'_{\boldsymbol{p}} - E_{\boldsymbol{p}}) \frac{d\sigma_{pb}^{NI}}{d\Omega}, \tag{3}$$

where the NIS differential cross section $\frac{d\sigma_{pb}^{NI}}{d\Omega}$ can be expressed as [35]

$$\frac{d\sigma_{pb}^{NI}(\mu, E_p)}{d\Omega} = P_{NI}(\mu, E_p)\sigma_{pb}^{NI}(E_p). \tag{4}$$

Here, $P_{NI}(\mu, E_p)$ is the angular distribution, where $\mu = \cos\Theta$ with Θ being the scattering angle in the center-of-mass system, and $\sigma_{pb}^{NI}(E_p)$ is the total cross section. On the experimental side, $\frac{d\sigma_{pb}^{NI}}{d\Omega}$ is defined by subtracting Coulomb contributions from the experimental data ($\frac{d\sigma_{pb}^{NI}}{d\Omega} = \frac{d\sigma_{pb}^{\exp}}{d\Omega} - \frac{d\sigma_{pb}^{\mathrm{Coul}}}{d\Omega}$). The NIS effect on the differential cross section has been clearly observed in the nuclear fusion experiments [58,59], and R-matrix calculations [35] are well consistent with the cross-section measurements. The energy change of the projectile particle after a two-body elastic collision in Eq. (3) is given by

$$\Delta E = E'_{\boldsymbol{p}} - E_{\boldsymbol{p}} = \tfrac{1}{2} m_p v_p'^2 - \tfrac{1}{2} m_p v_p^2, \tag{5}$$

where $\boldsymbol{v}'_p$ ($\boldsymbol{v}_p$) is the velocity of projectile particle after (before) the nuclear elastic scattering with the superscript "′" denoting the physical quantity after the elastic collision. By introducing the coordinate transformations $\boldsymbol{v}_{pC} \equiv \boldsymbol{v}_p - \boldsymbol{V}$, $\boldsymbol{v}_{bC} \equiv \boldsymbol{v}_b - \boldsymbol{V}$, $\boldsymbol{v}'_{pC} \equiv \boldsymbol{v}'_p - \boldsymbol{V}$, and $\boldsymbol{v}'_{bC} \equiv \boldsymbol{v}'_b - \boldsymbol{V}$, where $\boldsymbol{v}_b$ is the average thermal velocity of the plasma species b and

$$\boldsymbol{V} = \frac{m_p \boldsymbol{v}_p + m_b \boldsymbol{v} b}{m_p + m_b} \tag{6}$$

is the velocity in the center of mass system with the subscript C referring to the center-of-mass system, we have

$$\Delta E = -m_{pb} \boldsymbol{V} \cdot (\boldsymbol{v}_{pb} - \boldsymbol{v}'_{pb}). \tag{7}$$

The reduced mass of the projectile and plasma particles is defined as $m_{pb} = m_p m_b/(m_p + m_b)$, and the relative velocity is described by $v_{pb} = |\boldsymbol{v}_p - \boldsymbol{v}_b|$. Here, we have used the relationships that $|\boldsymbol{v}_{pC}| = |\boldsymbol{v}'_{pC}|$ and $|\boldsymbol{v}_{pb}| = |\boldsymbol{v}'_{pb}|$. Moreover, one can define $\boldsymbol{v}_{pb} = |\boldsymbol{v}_{pb}|\hat{e}_z$, the x-axis lies in the plane decided by $\boldsymbol{v}_p$ and $\boldsymbol{v}_b$, and the y-axis lies in the plane perpendicular to the one that decided by $\boldsymbol{v}_p$ and $\boldsymbol{v}_b$. After some algebraic transformation, we get

$$\Delta E = m_{pb}\left[\frac{\Delta E_{pb}}{m_p}(1 - \cos\Theta) + |\boldsymbol{V}||\boldsymbol{v}_{pb}| \sin\Theta \cos\Psi \sin\psi\right], \tag{8}$$

where ψ is the angle between $\boldsymbol{V}$ and $\boldsymbol{v}_{pb}$, (Θ, Ψ) is the spherical solid angle of $\boldsymbol{v}'_{pb}$, and

$$\Delta E_{pb} = m_{pb} v_{pb}^2 - m_p \boldsymbol{v}_p \cdot \boldsymbol{v}_{pb}. \tag{9}$$

Substituting this formula into Eq. (3) and finishing the integral of ψ from 0 to 2π, the contribution of NIS to the stopping power is rewritten as

$$\frac{dE^{NI}}{dx} = -\frac{1}{v_p} \sum_b \frac{m_{pb}}{m_p} \int \frac{d^3\boldsymbol{p}_b}{(2\pi\hbar)^3} f_b(\boldsymbol{p}_b) v_{pb} \times \int d\Omega \Delta E_{pb} (1 - \cos\Theta) \frac{d\sigma_{pb}^{NI}}{d\Omega}. \tag{10}$$

In addition, considering $\mathbf{v}_p \cdot \mathbf{v}_{pb} = v_p v_{pb} \cos\theta$, the distribution function is presented as

$$f_b(\boldsymbol{p}_b) = n_b (2\pi\beta_b/m_b)^{3/2} e^{-\frac{1}{2}\beta_b m_b \tilde{v}^2}, \tag{11}$$

where $\tilde{v}^2 = v_p^2 + v_b^2 + v_{pb}^2 - 2v_p v_{pb}\cos\theta$, and then Eq. (10) could be ulteriorly derived as

$$\frac{dE^{NI}}{dx} = \sum_b A_{NI} \int dv_{pb} \frac{v_{pb}^3}{v_p} f(v_p, v_{pb}) \sigma_{pb}^{tr}(v_{pb}), \tag{12}$$

where $A_{NI} = -(2\pi\beta_b m_b)^{1/2} m_{pb} n_b/\hbar^3$, the effective distribution function is

$$f(v_p, v_{pb}) = (1 + B_{NI}) e^{-v_+} + (1 - B_{NI}) e^{-v_-} \tag{13}$$

with $B_{NI} = \frac{m_p/(m_b\beta_b) + m_{pb} v_{pb}^2}{m_p v_p v_{pb}}$, and the transport cross section is expressed as

$$\sigma_{pb}^{tr}(v_{pb}) = \int_{-1}^{1} d\mu (1 - \mu) \frac{d\sigma_{pb}^{NI}(\mu, v_{pb})}{d\Omega}. \tag{14}$$

Notice that NIS contribution to the total stopping power is a non-Coulombic scattering term. This NIS contribution is different from the theoretical scheme in Refs. [60,61], in which the strong beam-plasma coupling effects are taken into account in the framework of the T-matrix approach, which describes the two-body interaction by the screened Coulomb potential.

III. NUMERICAL RESULTS AND ANALYSIS

A fundamental understanding of charged particle stopping in hot dense plasmas is essential to realizing fusion ignition. This requires accurate knowledge about the evolution of plasma conditions and the energy loss of charged particles in plasmas for a wide range of temperatures ranging from tens eV to 100 keV, and electron number densities from 10^{21} to 10^{26} cm^{-3} [15,21,22]. Based on these formulas, we numerically study the stopping power properties of fully ionized Be plasma for the proton. The differential NI cross-section $d\sigma_{pb}^{NI}(\mu, v_{pb})/d\Omega$ data of a proton with Be plasma are obtained from the international database package [36]. In this work, we consider the plasma temperature T changes from 10 keV to 100 keV, and the ion density of Be changes from 10^{24} to 10^{27} cm^{-3}. The projectile proton energy is about multi-MeV magnitude. The above parameters for the projectile proton and Be plasma are the specially concerned plasma condition for studies of ICF ignition, and could be realized under the present experimental technology. Therefore, the results obtained herein could be validated by the concerned experiments, and may be useful for the ICF studies.

From the international database package [36], we find the magnitude of $d\sigma_{p,Be}^{NI}/d\Omega$ is about 0.1 barn, which is much smaller than the Rutherford Coulomb cross section,

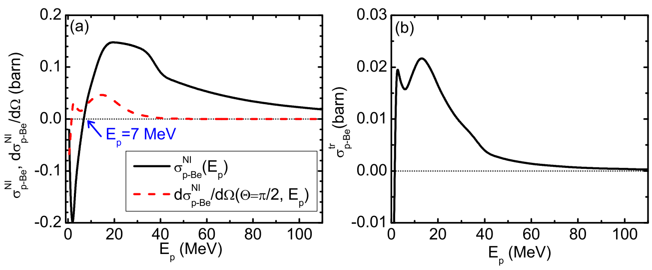

FIG. 1. (a) The total NI cross section $\sigma^{NI}_{p,Be}(E_p)$ (black solid line) and one special differential cross section $d\sigma^{NI}_{p,Be}/d\Omega(\Theta=\pi/2,E_p)$ (red dashed line) of proton traveling Be plasma vs. E_p. (b) The transport cross section $\sigma^{tr}_{p,Be}(E_p)$ (black solid line) as a function of E_p.

$d\sigma^{\mathrm{Coul}}/d\Omega = Z_p^2 Z_b^2 e^4/m_{pb}^2 v_{pb}^4 (1-\mu)^2$. Due to the interference effect, $d\sigma^{NI}_{p,Be}/d\Omega$ may be negative values in certain cases. Taking $\Theta=\pi/2$ as an example, we find the value of $d\sigma^{NI}/d\Omega(\Theta=\pi/2,E_p)$ is negative when E_p is smaller than 1 MeV. In Fig. 1(a), we plot the total cross section $\sigma^{NI}_{p,Be}(E_p)$ (black solid line) and its one special differential cross section $d\sigma^{NI}_{pb}/d\Omega(\Theta=\pi/2,E_p)$ (red dashed line) as functions of E_p. These characters of cross section may result in negative values in the stopping power. Furthermore, we also illustrate the transport cross section $\sigma^{tr}_{p,Be}(E_p)$ in Fig. 1(b) as a function of the energy of the projectile proton. From Fig. 1(b), one can see that there exits an oscillation near $E=7$ MeV since the remarkable interference effect, which may induce the oscillation in the stopping power as varying the velocity of the proton.

We show the stopping power of Be plasma with temperatures $T=10$ keV [see Fig. 2(a)] and $T=100$ keV [see Fig. 2(b)] as a function of the projectile proton's energy E_p. In Fig. 2, the black lines correspond to the CS part while the red dotted lines present the NIS contributions to the stopping power. In the calculations, the density of plasma is chosen as $n_{\mathrm{Be}}=10^{25}$ cm^{-3}. One can observe from Fig. 2 that oscillation phenomenon appears in the NIS part, and especially, one large valley appears near $E_p=7$ MeV, which is consistent with the behavior of the cross section near $E_p=7$ MeV shown in Fig. 1. Furthermore, the NIS part of the stopping power dE^{NI}/dx becomes negative when $E_p\approx 1$ MeV, which means that the proton is accelerated due to the NIS effect considered herein. In addition, in the case of $T=10$ keV, it is clear that the NIS scattering part is much smaller than the CS part, see Fig. 2(a). However, one can clearly see from Fig. 2 that with increasing the plasma temperature to $T=100$ keV, the CS part dE^{Coul}/dx decreases remarkably while the NIS part dE^{NI}/dx nearly keeps unchanged. Under this plasma condition, the ratio between NIS part and CS part,

$$\gamma = \frac{dE^{NI}/dx}{dE^{\mathrm{Coul}}/dx}, \quad (15)$$

increases from ~1% to ~10%. In other words, the NIS effect becomes important when the temperature of Be plasma is high to hundreds eV or much higher temperature. Using our formulas presented above, we have also calculated the stopping power of proton in the DT plasma. The numerical results are similar to those given by Mahdavi *et al.* in Ref. [46] and we do not show them here. We found that on one side, the NIS effect also becomes significant with increasing the temperature of DT plasma. On the other side, the NIS part dE^{NI}/dx will not exhibit oscillation phenomenon in the DT plasma, which is dramatically different from that in an Be plasma shown in this work.

It is clear that the NIS part is proportional to the density of plasma species, i.e., $dE^{NI}/dx \propto n_{\mathrm{Be}}$, see Eq. (12). Therefore, the NIS effect will be enhanced remarkably if we increase the density of plasma. The typical results of the radio between the NIS part and CS part, i.e., Eq. (15), as a function of E_p for different densities n_{Be} varying from 10^{24} to 10^{27} cm^{-3} are presented in Fig. 3. From Fig. 3, we find that, with the increase of density, the contribution of dE^{NI}/dx will be more significant than dE^{Coul}/dx on the stopping power of the projectile. Therefore, in the dense plasmas, such as the ICF plasmas, NIS effect plays an significant role on the stopping power of projectiles. There are at least two additional things need to

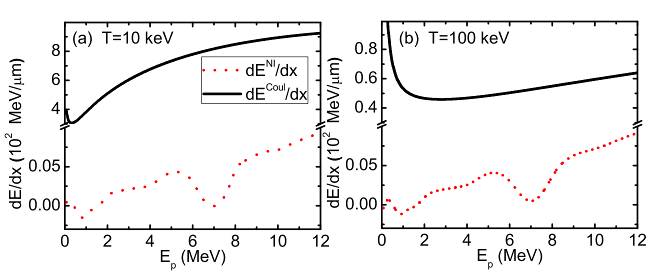

FIG. 2. Stopping power dE/dx of proton projectile moving fully ionized Be plasma with temperatures (a) $T=10$ keV and (b) $T=100$ keV. The black solid line and the red dotted line correspond to the CS part dE^{Coul}/dx and the NIS part dE^{NI}/dx, respectively. The density of Be ion species is chosen as $n_{Be}=10^{25}$ cm^{-3}.

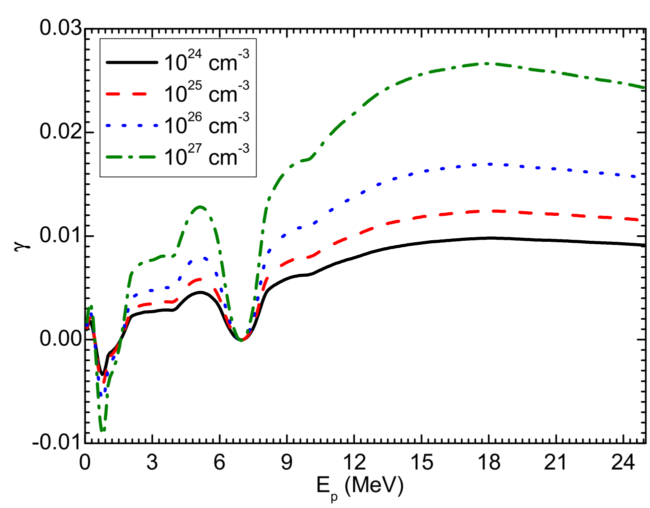

FIG. 3. Ratio between NIS stopping power dE^{NI}/dx and CS stopping power dE^{Coul}/dx for proton projectile moving in Be plasma as a function of energy E_p. In the calculations, several plasma number densities are chosen as $n_{\mathrm{Be}}=10^{24}$ cm^{-3} (black solid line), $n_{\mathrm{Be}}=10^{25}$ cm^{-3} (red dashed line), $n_{\mathrm{Be}}=10^{26}$ cm^{-3} (blue dotted line), and $n_{\mathrm{Be}}=10^{27}$cm^{-3} (olive dash-dotted line), and the temperature is chosen as $T=10$ keV.

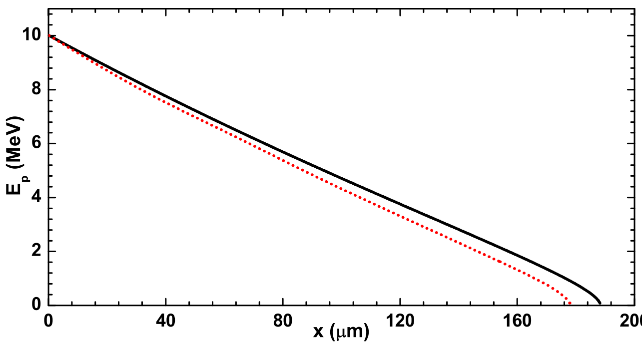

FIG. 4. The penetration of proton with initial energy $E_p = 10$ MeV in the Be plasma with $n_{\mathrm{Be}} = 10^{25}$ cm^{-3}, and $T = 100$ keV. The red dotted line (black solid line) corresponds to the result in the presence (absence) of NIS effect in the calculations.

noticed. For one thing, when $E_p = 1.6$ and 7 MeV, γ tends to vanish since the cross section $d\sigma^{NI}/d\Omega$ obtained from the international database package [36] equals to zero. This may be a special nuclear scattering and interference phenomenon for Be plasma; For another thing, consistent with the result of the cross section shown in Fig. 1, when $E_p < 1.6$ MeV, γ becomes negative. Additionally, the ratio between NIS part and CS part approaches the maximum value when the energy of proton E_p increases up to 18 MeV, see Fig. 3.

The physical qualities related to the stopping power, such as penetration distance of charged particles, should be accurately estimated if the NIS effect is taken into account in the calculations. The penetration distance x that a proton projectile, starting with energy E_0, is slowed down to reach the energy E is given by

$$x(E,E_0) = \int_E^{E_0} dE \left(\frac{dE}{dx}\right)^{-1}. \tag{16}$$

As an example, we numerically calculate the penetration distance of proton with initial energy $E_p = 10$ MeV in the Be plasma with $n_{\mathrm{Be}} = 10^{25}$ cm^{-3} and $T = 100$ keV. The corresponding numerical results are shown in Fig. 4. In the absence of the NIS effect in the calculation, the obtained penetration distance is $x = 188$ μm (see black solid line in Fig. 4). While in the presence of the NIS effect, the penetration distance is reduced to $x = 178$ μm (see red dotted line in Fig. 4). We see that the NIS should be of importance for multi-MeV charged particles moving in the plasmas with high temperature and dense density. This NIS effect accelerates the slowing-down process and shortens the penetration distance, and thus enhances the heating of background ions.

The pure Coulomb cross section is analytically expressed by using the Rutherford formula, and it can be subtracted from the total scattering cross section. The other part of the total scattering cross section, i.e., the NI cross section is suggested as Eq. (4), or a polynomial expansion [35]. The NI cross section for protons on Be nuclei has been experimentally measured, see Ref. [36]. Presently, the validity of BPS model for pure Coulomb interaction has been quantitatively checked in the ion-stopping experiment performed at the OMEGA laser facility [15]. It has been proven that spectrally resolved x-ray scattering [62] should be an outstanding tool to characterize dense plasma parameters. Recent experiments at the OMEGA laser facility of University of Rochester on directly driven beryllium capsule could investigate electron densities up to 10^{24} cm^{-3} [63] and electron temperatures up to tens keV [15,64]. With the availability of the National Ignition Facility (NIF), these studies can be extended to much higher densities and temperatures. Most recently, Kraus *et al.* [49] reported that the platform for spectrally resolved x-ray scattering from imploding capsules at NIF has been constructed. This platform will allow for the studies of hot dense plasmas with electron densities approaching and eventually exceeding 10^{25} cm^{-3}. The researchers at NIF plan to perform the experimental measurements using Be capsules to achieve the extreme plasma conditions. Therefore, this platform at NIF [49–51] may give the possibility to study the NIS effect during the implosion in the future.

Moreover, Shuy and Conn pointed out that [65] the fusion reaction cross sections and reaction rate parameters are likewise influenced by NIS effect, and the reactivity of advanced fusion fuels could be enhanced by taking into account the NIS effect. Perkins and Cullen estimated that [66] the NIS may approach zero for projectile energies in or near the energy range from B_L to $B_L/10$, where B_L is the laboratory Coulomb barrier energy. The data given in Refs. [66,67] allow one to calculate both the rate at which particles interact and the rate at which they lose energy due to NIS effect. Of particular interest for our concern in this work is the $^6\mathrm{Li} + {}^3\mathrm{He} \to p + {}^8\mathrm{Be}$ fusion reaction, where ^{8}Be can be in different energy states [66]. The fusion reaction products, such as proton particles, are energetic and may react with elements in the background plasma prior to completely slowing down. NIS between the energetic products and the background plasma products additionally heats particles which can undergo fast fusion and further propagate the reaction. The maximum ratio between the NIS part and CS part occurs when the proton energy is up to 18 MeV, see Fig. 3. Therefore, the influence of NIS on the reaction cross section for the various channels may be also significantly enhanced by the energetic protons with energy about ∼20 MeV [65,66].

IV. SUMMARY

In summary, we have theoretically investigated the NIS effect on the stopping power of hot dense Be plasmas for multi-MeV protons. The analytical expression of the NIS stopping power was carefully derived, and the BPS model was generalized. By applying this generalized BPS formula, we numerically showed the NIS effect on the stopping power of proton moving in the Be plasma. The results show that with increasing the plasma temperature and/or the number density, the NIS effect will be enhanced. As a result, the penetration distance of charged particles in the hot dense plasmas, may be remarkably affected by the NIS effect. Different from the cases of protons traveling through the DT plasmas, a prominent oscillation valley structure is observed in the NIS term of the stopping power of the Be plasma for protons as a function of the proton's energy near $E_p = 7$ MeV. The maximum ratio between NIS part and CS part occurs when the proton energy is up to 18 MeV. Furthermore, the penetration distance is reduced due to the NIS effect.

ACKNOWLEDGMENTS

This work was supported by National Natural Science Foundation of China under Grants No. 11575032, No. 11675023, No. 11274049, No. 11304009, and No. U1530258, by the President Foundation of China Academy of Engineering Physics (CAEP) under Grant No. YZ2015014, by the Foundation for the Development of Science and Technology of CAEP under Grant No. 2014B0102015, and by the National Magnetic Confinement Fusion Energy Research Project of China under Grant No. 2015B108002.

Z.W. and Z.F. contributed equally to this work.

[1] M. W. C. Dharma-wardana, in *Laser Interactions with Atoms, Solids, and Plasmas*, NATO Advanced Study Institutes, Series B Vol. 327, edited by R. M. More (Plenum, New York, 1994), p. 331.

[2] N. Bohr, Phil. Mag. **25**, 10 (1913).

[3] H. Bethe, Ann. Phys. (NY) **397**, 325 (1930); F. Bloch, *ibid.* **408**, 285 (1933).

[4] T. A. Mehlhorn, J. Appl. Phys. **52**, 6522 (1981); G. Zimmerman, LLNL, Report No. UCRL-JC-105616 (1990); I. Nagy and B. Apagyi, Phys. Rev. A **58**, R1653 (1998); G. Faussurier, C. Blancard, P. Cossé, and P. Renaudin, Phys. Plasmas **17**, 052707 (2010).

[5] L. S. Brown, D. L. Preston, and R. L. Singleton, Jr., Phys. Rep. **410**, 237 (2005).

[6] M. W. C. Dharma-wardana and F. Perrot, Phys. Rev. E **58**, 3705 (1998); **63**, 069901(E) (2001); M. W. C. Dharma-wardana, Phys. Rev. Lett. **101**, 035002 (2008).

[7] J. Daligault and G. Dimonte, Phys. Rev. E **79**, 056403 (2009).

[8] M. D. Barriga-Carrasco, Phys. Rev. E **79**, 027401 (2009).

[9] Z.-G. Fu, Z. Wang, D.-F. Li, W. Kang, and P. Zhang, Phys. Rev. E **92**, 033103 (2015).

[10] G. Hazak, Z. Zinamon, Y. Rosenfeld, and M. W. C. Dharma-wardana, Phys. Rev. E **64**, 066411 (2001).

[11] P. Sigmund, R. Bimbot, H. Geissel, H. Paul, and A. Schinner, *Stopping of Ions Heavier than Helium*, ICRU Report, Vol. 73 (Oxford University Press, Oxford, 2005).

[12] H. Paul, Nucl. Instrum. Methods Phys. Res. B **247**, 166 (2006).

[13] A. B. Zylstra, C. K. Li, H. G. Rinderknecht, F. H. Séguin, R. D. Petrasso, C. Stoeckl, D. D. Meyerhofer, P. Nilson, T. C. Sangster, S. Le Pape *et al.*, Rev. Sci. Instrum. **83**, 013511 (2012).

[14] A. B. Zylstra, J. A. Frenje, P. E. Grabowski, C. K. Li, G. W. Collins, P. Fitzsimmons, S. Glenzer, F. Graziani, S. B. Hansen, S. X. Hu *et al.*, Phys. Rev. Lett. **114**, 215002 (2015).

[15] J. A. Frenje, P. E. Grabowski, C. K. Li, F. H. Séguin, A. B. Zylstra, M. Gatu Johnson, R. D. Petrasso, V. Yu Glebov, and T. C. Sangster, Phys. Rev. Lett. **115**, 205001 (2015).

[16] A. Frank, A. Blažević, V. Bagnoud, M. M. Basko, M. Börner, W. Cayzac, D. Kraus, T. Heßing, D. H. H. Hoffmann, A. Ortner *et al.*, Phys. Rev. Lett. **110**, 115001 (2013).

[17] W. Cayzac, V. Bagnoud, M. M. Basko, A. Blažević, A. Frank, D. O. Gericke, L. Hallo, G. Malka, A. Ortner, An. Tauschwitz *et al.*, Phys. Rev. E **92**, 053109 (2015).

[18] B. Yu. Sharkov, D. G. Koshkarev, M. D. Churazov, N. N. Alexeev, M. M. Basko, A. A. Golubev, and P. R. Zenkevich, Nucl. Instrum. Methods Phys. Res. A **415**, 20 (1998).

[19] C. K. Li and R. D. Petrasso, Phys. Rev. Lett. **70**, 3059 (1993); **114**, 199901(E) (2015).

[20] A. Golubev, M. Basko, A. Fertman, A. Kozodaev, N. Mesheryakov, B. Sharkov, A. Vishnevskiy, V. Fortov, M. Kulish, V. Gryaznov *et al.*, Phys. Rev. E **57**, 3363 (1998).

[21] J. D. Lindl, *Inertial Confinement Fusion: The Quest for Ignition and Energy Gain Using Indirect Drive* (Springer-Verlag, New York, 1998).

[22] G. H. Miller, E. I. Moses, and C. R. Wuest, Nucl. Fusion **44**, S228 (2004).

[23] J. Jacoby, D. H. H. Hoffmann, W. Laux, R. W. Müller, H. Wahl, K. Weyrich, E. Boggasch, B. Heimrich, C. Stöckl, H. Wetzler, and S. Miyamoto, Phys. Rev. Lett. **74**, 1550 (1995).

[24] J. R. Rygg, F. H. Séguin, C. K. Li, J. A. Frenje, M. J. E. Manuel, R. D. Petrasso, R. Betti, J. A. Delettrez, O. V. Gotchev, J. P. Knauer *et al.*, Science **319**, 1223 (2008).

[25] P. A. Norreys, Science **327**, 1208 (2010).

[26] S. H. Glenzer, B. J. MacGowan, P. Michel, N. B. Meezan, L. J. Suter, S. N. Dixit, J. L. Kline, G. A. Kyrala, D. K. Bradley, D. A. Callahan *et al.*, Science **327**, 1228 (2010).

[27] C. K. Li, F. H. Séguin, J. A. Frenje, M. Rosenberg, R. D. Petrasso, P. A. Amendt, J. A. Koch, O. L. Landen, H. S. Park, H. F. Robey *et al.*, Science **327**, 1231 (2010).

[28] J. A. Frenje, C. K. Li, F. H. Séguin, D. T. Casey, R. D. Petrasso, D. P. McNabb, P. Navratil, S. Quaglioni, T. C. Sangster, V. Yu Glebov *et al.*, Phys. Rev. Lett. **107**, 122502 (2011).

[29] T. Döppner, C. A. Thomas, L. Divol, E. L. Dewald, P. M. Celliers, D. K. Bradley, D. A. Callahan, S. N. Dixit, J. A. Harte, S. M. Glenn *et al.*, Phys. Rev. Lett. **108**, 135006 (2012).

[30] S. P. Regan, R. Epstein, B. A. Hammel, L. J. Suter, H. A. Scott, M. A. Barrios, D. K. Bradley, D. A. Callahan, C. Cerjan, G. W. Collins *et al.*, Phys. Rev. Lett. **111**, 045001 (2013).

[31] T. Ma, P. K. Patel, N. Izumi, P. T. Springer, M. H. Key, L. J. Atherton, L. R. Benedetti, D. K. Bradley, D. A. Callahan, P. M. Celliers *et al.*, Phys. Rev. Lett. **111**, 085004 (2013).

[32] O. L. Landen, T. R. Boehly, D. K. Bradley, D. G. Braun, D. A. Callahan, P. M. Celliers, G. W. Collins, E. L. Dewald, L. Divol, S. H. Glenzer *et al.*, Phys. Plasmas **17**, 056301 (2010).

[33] C. K. Li, F. H. Séguin, J. A. Frenje, M. J. Rosenberg, H. G. Rinderknecht, A. B. Zylstra, R. D. Petrasso, P. A. Amendt, O. L. Landen, A. J. Mackinnon *et al.*, Phys. Rev. Lett. **108**, 025001 (2012).

[34] Z. Wang, Z.-G. Fu, B. He, and P. Zhang, Phys. Plasmas **21**, 072703 (2014); **21**, 102307 (2014).

[35] A. Andrade and G. M. Hale, Phys. Rev. A **30**, 1940 (1984).

[36] M. B. Chadwick, M. Herman, P. Oblozinsky, M. E. Dunn, Y. Danon, A. C. Kahler, D. L. Smith, B. Pritychenko, G. Arbbnas, R. Arcilla *et al.*, Nucl. Data Sheets **112**, 2887 (2011).

[37] J. J. Devaney and M. L. Stein, Nucl. Sci. Eng. **46**, 323 (1971).

[38] M. Tabak, J. Hammer, M. E. Glinsky, W. L. Kruer, S. C. Wilks, J. Woodworth, E. M. Capbell, M. D. Perry, and R. J. Mason, Phys. Plasmas **1**, 1626 (1994).

[39] J. A. Delettrez, J. Myatt, P. B. Radha, C. Stoeckl, S. Skupsky, and D. D. Meyerhofer, Plasma Phys. Controlled Fusion **47**, B791 (2005).

[40] N. Miyanaga, H. Azechi, K. A. Tanaka, T. Kanabe, T. Jitsuno, Y. Fujimoto, R. Kodama, H. Shiraga, K. Kondo, K. Tsubakimoto *et al.*, in *Inertial Fusion Sciences and Applications 2003*, edited by B. Hammel, D. D. Meyerhofer, J. Meyer-ter-Vehn, and H. Azechi (American Nuclear Society, Lagrange Park, 2004), p. 507.

[41] M. Dunne, Nat. Phys. **2**, 2 (2006).

[42] M. Dunne, N. Alexander, F. Amiranoff, P. Aguer, S. Atzeni, H. Azechi, V. Bagnoud, P. Balcou, J. Badziak, D. Batani *et al.*, HiPER-Technical Background and Conceptual Design Report, Report No. RAL-TR-2007-008 (Rutherford Appleton Laboratory, Didcot, UK, 2007).

[43] C. Deutsch, H. Furukawa, K. Mima, M. Murakami, and K. Nishihara, Phys. Rev. Lett. **77**, 2483 (1996); **85**, 1140(E) (2000).

[44] C. K. Li and R. D. Petrasso, Phys. Rev. E **70**, 067401 (2004).

[45] C. K. Li and R. D. Petrasso, Phys. Rev. E **73**, 016402 (2006); Phys. Plasmas **13**, 056314 (2006).

[46] M. Mahdavi and T. Koohrokhi, Mod. Phys. Lett. A **26**, 1561 (2011); Phys. Rev. E **85**, 016405 (2012).

[47] M. Mahdavi, T. Koohrokhi, and R. Azadifar, Phys. Plasmas **19**, 082707 (2012).

[48] F. Wagner, O. Deppert, C. Brabetz, P. Fiala, A. Kleinschmidt, P. Poth, V. A. Schanz, A. Tebartz, B. Zielbauer, M. Roth *et al.*, Phys. Rev. Lett. **116**, 205002 (2016).

[49] D. Kraus, D. A. Chapman, A. L. Kritcher, R. A. Baggott, B. Bachmann, G. W. Collins, S. H. Glenzer, J. A. Hawreliak, D. H. Kalantar, O. L. Landen *et al.*, Phys. Rev. E **94**, 011202(R) (2016).

[50] A. L. Kritcher, T. Döppner, D. Swift, J. Hawreliak, G. Collins, J. Nilsen, B. Bachmann, E. Dewald, D. Strozzi, S. Felker *et al.*, High Energy Density Phys. **10**, 27 (2014).

[51] T. Döppner, A. L. Kritcher, D. Kraus, S. H. Glenzer, B. L. Bachmann, D. Chapman, G. W. Collins, R. W. Falcone, J. Hawreliak, O. L. Landen *et al.*, J. Phys.: Conf. Ser. **500**, 192019 (2014).

[52] S. Atzeni and J. Meyer-ter-Vehn, *The Physics of Inertial Fusion: Beam Plasma Interaction, Hydrodynamics, Hot Dense Matter, International Series of Monographs on Physics* (Clarendon Press, Oxford, 2004).

[53] A. Macchi, M. Borghesi, and M. Passoni, Rev. Mod. Phys. **85**, 751 (2013), and references therein.

[54] D. T. Michel, V. N. Goncharov, I. V. Igumenshchev, R. Epstein, and D. H. Froula, Phys. Rev. Lett. **111**, 245005 (2013).

[55] S. A. Yi, A. N. Simakov, D. C. Wilson, R. E. Olson, J. L. Kline, D. S. Clark, B. A. Hammel, J. L. Milovich, J. D. Salmonson, B. J. Kozioziemski, and S. H. Batha, Phys. Plasmas **21**, 092701 (2014).

[56] D. T. Casey, D. T. Woods, V. A. Smalyuk, O. A. Hurricane, V. Y. Glebov, C. Stoeckl, W. Theobald, R. Wallace, A. Nikroo, M. Schoff *et al.*, Phys. Rev. Lett. **114**, 205002 (2015).

[57] R. K. Follett, J. A. Delettrez, D. H. Edgell, V. N. Goncharov, R. J. Henchen, J. Katz, D. T. Michel, J. F. Myatt, J. Shaw, A. A. Solodov *et al.*, Phys. Rev. Lett. **116**, 155002 (2016).

[58] M. Ivanovich, P. G. Young, and G. G. Ohlsen, Nucl. Phys. A **110**, 441 (1968).

[59] A. S. Wilson, M. C. Taylor, J. C. Legg, and G. C. Phillips, Nucl. Phys. A **126**, 193 (1969).

[60] W. D. Kraeft and B. Strege, Physica A **149**, 313 (1988).

[61] D. O. Gericke and M. Schlanges, Phys. Rev. E **60**, 904 (1999).

[62] S. H. Glenzer and R. Redmer, Rev. Mod. Phys. **81**, 1625 (2009).

[63] A. L. Kritcher, T. Döppner, C. Fortmann, T. Ma, O. L. Landen, R. Wallace, and S. H. Glenzer, Phys. Rev. Lett. **107**, 015002 (2011).

[64] S. H. Glenzer, G. Gregori, F. J. Rogers, D. H. Froula, S. W. Pollaine, R. S. Wallace, and O. L. Landen, Phys. Plasmas **10**, 2433 (2003).

[65] G. W. Shuy and R. W. Conn, *Charged Particle Cross-Section Requirements for Advanced Fusion Cycles*, presented at the APS International Conference on Nuclear Cross Sections for Technology (Knocwille, 1979), pp. 22–26.

[66] S. T. Perkins and D. E. Cullen, Nucl. Sci. Eng. **77**, 20 (1981).

[67] D. E. Cullen and S. T. Perkins, Conservation of Reaction Rate and Average Rate of Energy Loss in Charged Particle Transport Calculations, UCRL-84845, Lawrence Livermore National Laboratory (1980).